AGU PUBLICATIONS

Geophysical Research Letters

RESEARCH LETTER
10.1002/2015GL065047

Key Points:
- There are two distinct types of highly energetic IC lightning in thunderstorms
- The new type occurs at 10–13 km altitude during leader propagation
- There is a connection between the new type and TGFs

Correspondence to:
S. A. Cummer,
cummer@ee.duke.edu

Citation:
Lyu, F., S. A. Cummer, and L. McTague (2015), Insights into high peak current in-cloud lightning events during thunderstorms, *Geophys. Res. Lett.*, *42*, 6836–6843, doi:10.1002/2015GL065047.

Received 22 JUN 2015
Accepted 30 JUL 2015
Accepted article online 31 JUL 2015
Published online 22 AUG 2015

Insights into high peak current in-cloud lightning events during thunderstorms

Fanchao Lyu[1], Steven A. Cummer[1], and Lindsay McTague[1]

[1]Electrical and Computer Engineering Department, Duke University, Durham, North Carolina, USA

Abstract We investigated National Lightning Detection Network reports and lightning radio waveforms in a 44 day observation period to analyze the in-cloud (IC) events producing currents above 200 kA. The results show that there are two distinct classes of IC lightning events with very high peak currents: the well-known narrow bipolar events, and a previously unreported type that we call energetic in-cloud pulses (EIPs). Their temporal and spatial context shows that EIPs are generated from existing negative polarity leaders that are propagating usually upward but sometimes downward. The nearly identical characteristics of EIPs and some previously reported terrestrial gamma ray flashes (TGFs) indicate a likely connection between the two, which further suggests the possibility of downward directed TGFs. These very high peak current IC events also suggest the association of EIPs with ionospheric perturbations and optical emissions known as elves.

1. Introduction

Lightning in thunderstorms produce broadband electromagnetic emission over a wide amplitude and energy range. Studies of high-energy atmospheric discharge processes give important insight into lightning initiation as well as the relationship between such energetic discharges and other associated discharge phenomena [*Dwyer et al.*, 2012]. Energetic lightning discharges during thunderstorms, such as cloud-to-ground (CG) lightning discharges with large charge moment change (CMC) [*Cummer and Lyons*, 2004] or high peak current (I_{pk}), are known to be responsible for the production of brief, but gigantic, optical emissions above the thundercloud [*Inan et al.*, 2010], such as sprites [*Franz et al.*, 1990] or elves [*Inan et al.*, 1991; *Fukunishi et al.*, 1996].

Although CG strokes account for the majority of the most powerful discharges, previous studies have shown that some in-cloud (IC) events can produce highly energetic radio frequency (RF) emissions. Lightning narrow bipolar events (NBEs), or compact intracloud discharges (CIDs), were reported to produce powerful natural RF emissions with very short pulse duration [*Le Vine*, 1980; *Smith et al.*, 1999]. NBEs were also considered to be associated with the initiation of some IC flashes [*Rison et al.*, 1999; *Wu et al.*, 2014], although, notably, the physical mechanism of NBEs is still unclear. The bimodal distribution of the impulse charge moment change (iCMC) for high I_{pk} lightning events [*Cummer et al.*, 2013] has suggested that some other IC events may also be capable of producing the high-amplitude RF emissions that are associated with high I_{pk}. A few recently reported IC events with National Lightning Detection Network (NLDN) I_{pk} above 100 kA were associated with terrestrial gamma ray flashes (TGFs) [*Lu et al.*, 2011; *Cummer et al.*, 2014]. TGFs [*Fishman et al.*, 1994] are brief bursts of energetic gammy ray photons in the Earth's atmosphere that can be detected by satellite-based detectors [*Smith et al.*, 2005; *Briggs et al.*, 2010]. Whether these IC events are responsible for TGFs or are a by-product of the production of TGFs is still an open question.

It is valuable to conduct more studies on the phenomenon of energetic lightning, especially pertaining to energetic IC lightning events, as well as the relationship between the energetic ICs and other associated events. Thus, a basic question arises with the energetic lightning study: in addition to CG strokes, what kinds of IC events could produce very high I_{pk} during thunderstorms? Similarly, are there any specific characteristics of these ICs, and is there any relationship between these kind of events and other normal lightning events or other phenomena associated with the thunderstorms? These questions are the focus of this study.

We analyzed the lightning sferics associated with NLDN-reported very high I_{pk} (≥200 kA) lightning events to investigate the types of highly energetic IC lightning events that occur during thunderstorms. NLDN provides the time, location, types, peak current, event polarity, and other parameters of CGs and ICs in the United States [*Cummins et al.*, 1998; *Cummins and Murphy*, 2009]. However, there is limited information on the details

of IC events. The lightning sferics continuously recorded by Duke low frequency (LF) magnetic sensor network, which have been widely used in previous studies of transient luminous events [e.g., *Lu et al*., 2013], provided more details on the types of discharges and the temporal context of particular discharges with neighboring events through post processing. We recognize that the NLDN-reported I_{pk} is effectively a scaled and normalized peak radiated electric field. While it has been empirically calibrated for some classes of CG lightning [*Cummins et al*., 1998], it may have little connection to the actual peak current in an IC lightning event. Nevertheless, NLDN I_{pk} is a simple and effective way for identifying highly energetic IC lightning events, and a 200 kA lightning event is energetic by just about any metric.

After removing cloud-to-ground strokes from the event database, we find that there are two distinct and separable types of IC lightning events that are reported by the NLDN having peak current above 200 kA. One is the well known, but poorly understood, NBE. The other is class of slower waveforms that occur in a very different lightning context, which we refer to as energetic in-cloud pulses (EIPs). Below, we show the differences between NBE and EIP waveforms. We show via a source altitude analysis that EIPs are produced during upward (usually) and downward (sometimes) negative-polarity lightning leader propagation and discuss the possible connections between EIPs, TGFs, and elves.

2. Data Summary and Event Identification

Our data set is formed using NLDN data [*Cummins et al*., 1998] and lightning sferic waveforms recorded at multiple lightning sensor stations over 44 days (3 September to 16 October 2014). We begin with all NLDN lightning events reported as ICs with I_{pk} greater than 200 kA and that occurred within 1000 km of an operating LF sensor in Duke magnetic sensor network. Five LF sensors, deployed in Durham, NC (Duke), Oxford, MS (Miss), Melbourne, FL (FIT), Norman, OK (OU), and Manhattan, KS (KSU), are involved in this study. This resulted in 199 lightning events that met the criteria. We also folded into the data set the signals for these events as recorded by GPS-synchronized very low frequency (VLF, 50 Hz to ~30 kHz) and ultralow frequency (ULF, $<$1 Hz to 400 Hz) magnetic sensors [*Lu et al*., 2013] operating near Duke University.

The LF/VLF/ULF sferic data enabled us to classify lightning events in postprocessing with minimal ambiguity. Some of the NLDN-identified IC events were actually CG strokes when we visually analyzed their sferic waveforms. The final classification of these events was confirmed by cooperation with Vaisala, Inc. (K. Cummins and A. Nag, personal communication, 2015). After the careful examination of the sferic waveforms, these 199 very high I_{pk} events were split into 59 negative CGs (−CGs), 1 positive CG (+CG), and 139 ICs.

An initial visual inspection indicated that these 139 ICs could be divided into two different IC types. Some of these were clearly NBEs [*Le Vine*, 1980; *Smith et al*., 1999], which have very short pulse duration, extremely short risetime, are usually relatively isolated from other IC events [*Smith et al*., 1999], and have been reported and analyzed in many papers. But there is also a second group of pulses that appear to be significantly longer duration than NBEs. Furthermore, these pulses are not isolated, but instead, typically are associated with smaller discrete pulses that occur within a several millisecond time window. Paired ionospheric reflections from these pulses confirm that they are elevated discharges above the ground [*Smith et al*., 1999, 2004]. We will henceforth refer to these IC events as energetic in-cloud pulses (EIPs).

Among all the 139 sferic-identified IC events, there were 67 negative NBEs (−NBEs), 69 positive EIPs (+EIPs), and 3 negative EIPs (−EIPs) according to visual waveform classification. Figure 1a shows examples of the LF waveforms associated with the different types of NLDN-identified events (including both sferic-identified CGs and ICs) that have $I_{pk} \geq 200$ kA in the original 199 events. The longer time scale and lack of isolation make EIPs clearly distinct from NBEs.

EIPs, NBEs, and CGs can be quantitatively distinguished based on certain characteristics of their LF waveforms. This is not necessarily meant to be the optimal method of distinguishing between them but is meant to show that they can be distinguished reliably and automatically. We first define several waveform features. As shown in Figure 1b, Point A is 10% of the maximum of the initial pulse that A precedes. B is 10% of the maximum peak of the main pulse in AB. C is the point having the same absolute value as B within the window after B but before the ionosphere reflections. Point C is used to account for multiple overshoots for the events. For the events that do not have decent multiple overshoots, point C is the same as point B. BD indicates a 20 μs time window containing the sferic activity after B; AE indicates a 500 μs time window before A.

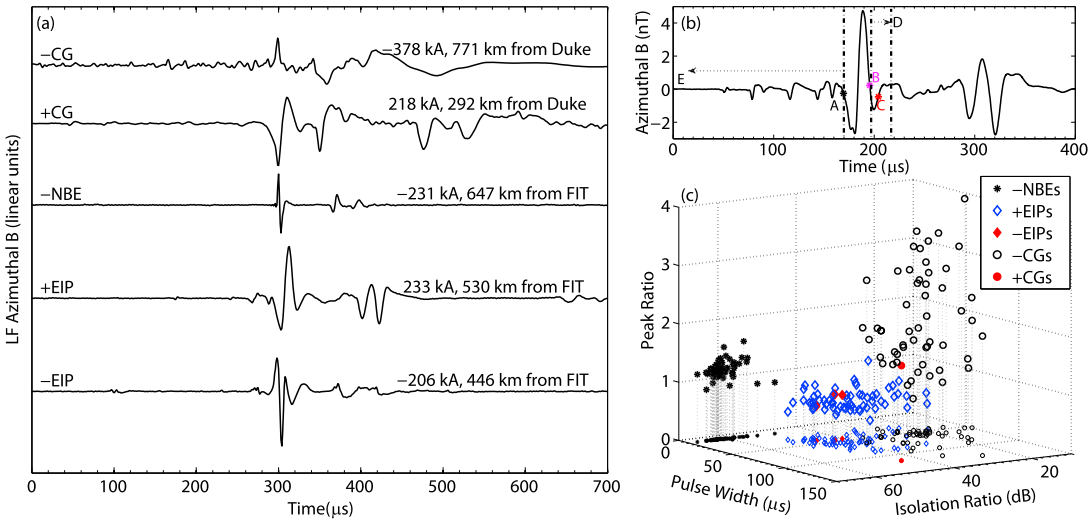

Figure 1. (a) Different polarities of lightning discharge types that produced ultrahigh I_{pk} in a time window of 0.7 ms. The event discharge polarity is determined from the initial polarity of main azimuthal magnetic field (*B*) pulse, as illustrated by the figure texts. (b) Definition of the LF waveform parameters used in the event identification. (c) Three-dimensional scatterplot of the three parameters for 67 −NBEs (black asterisk), 66 +EIPs (blue diamond), 3 –EIPs (red filled diamond), 54 −CGs (black circle), and one +CG (red filled circle). The dotted line and the smaller signs illustrate the projection of different events onto the horizontal plane.

We then define three parameters for the discrimination of these events: (1) pulse width (the time duration of AC); (2) peak ratio, the initial peak to the overshoot peak of the main pulse in AB; and (3) isolation ratio, the sum of preceding and post activity ratio. Activity ratio is defined as $10\times\log_{10}\left[\frac{1}{M}\left(\sum_{i=1}^{M} B_i^2\right)/\frac{1}{N}\left(\sum_{j=1}^{N} B_j^2\right)\right]$, B_i ($i=1, \ldots, M$) is the LF signals in window AB, for preceding activity ratio, B_j ($j=1,\ldots, N$) is the LF signals in window AE, for post activity ratio, B_j ($j=1,\ldots, N$) is the LF signals in window BD, as shown in Figure 1b.

We compute these three parameters for those events with *clear* LF waveforms, which were composed of 67 −NBEs, 66 +EIPs, 3 −EIPs, 54 −CGs, and 1 +CG. The mean pulse width for CGs, NBEs, and EIPs is 61.3 μs, 9.2 μs, and 55.1 μs, respectively. The mean peak ratio for CGs, NBEs, and EIPs is 2.5, 1.2, and 0.7, respectively. And, the mean value of isolation ratio for CGs, NBEs, and EIPs is 24.6 dB, 61.5 dB, and 40.4 dB, respectively. As illustrated in Figure 1c, these three types of events are separated in different groups, demonstrating the type differences in themselves. These parameters can also serve as a potential event classification reference in future data investigation.

All 67 −NBEs produced NLDN I_{pk} ranging from 200 kA to 304 kA and had a mean of 228.9 kA. The I_{pk} of 72 EIPs ranged from 200 kA to 584 kA, with a mean of 273.9 kA. Despite the very high I_{pk} for these NBEs and EIPs, they produced only modest iCMCs measured from the Charge Moment Change Network (CMCN) [*Cummer et al.*, 2013]. Specifically, the EIPs produced iCMC ranges from 1 to 53 C km, with a mean iCMC of 19.5 C km. The iCMC of the NBEs was too small to be measured by the CMCN. This indicates that misidentified IC events might form the population of high I_{pk}/low iCMC positive polarity events identified in *Cummer et al.* [2013]. Of the 67 −NBEs, 51 of them were clustered during three storms. In contrast, nearly all the 72 EIPs were produced by different storms. −NBEs tend to cluster in some particularly strong storms [*Wiens et al.*, 2008], while our data suggest that EIPs do not cluster and randomly distribute in different storms. The phenomenology and the context of NBEs have been discussed by many researchers, so the main work of this study focuses on EIPs, as well as initial comparison between EIPs and NBEs.

3. NBEs and EIPs Source Altitude and Meteorological Context Within Thunderstorms

The source altitude of the events relative to thunderstorms indicates the meteorological context of the events. LF signals that propagate within the Earth-ionosphere waveguide can be reflected by the Earth and the ionosphere. The altitude of the emission's source and virtual ionosphere can be retrieved from the time intervals between two reflections and the ground wave [*Smith et al.*, 2004]. A total of 90 events,

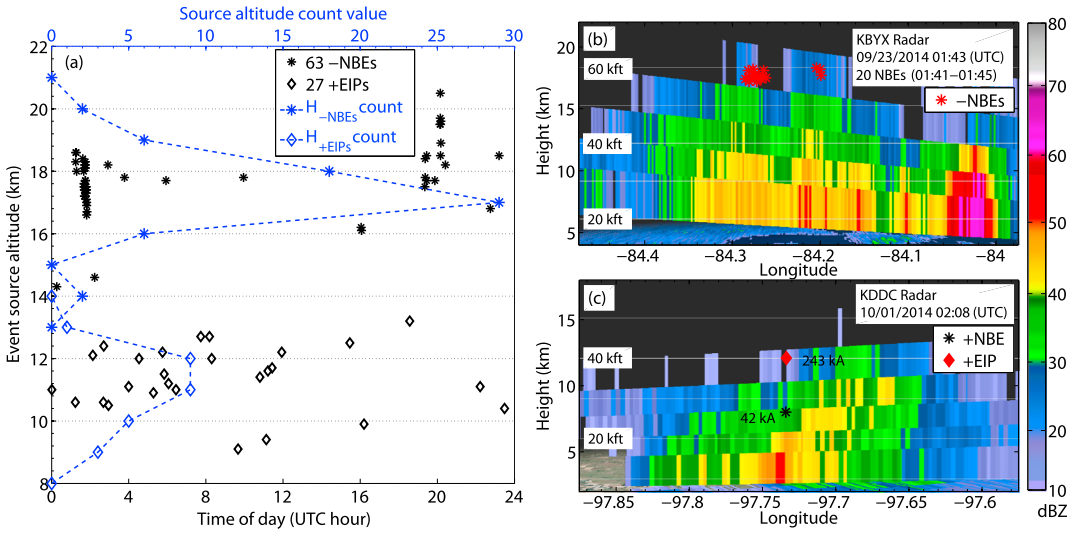

Figure 2. (a) Source altitude of 63 −NBEs (black asterisk), 27 +EIPs (black diamond) versus time of day (UTC hour) as labeled by the black bottom axis, and the event source altitude distribution of −NBEs (blue star-dashed line) and +EIPs (blue diamond-dashed line) as labeled by the top blue axis. (b) Source altitude of 20 NBEs (red asterisk) during 01:41–01:45 UTC and the vertical profile of radar echo at 01:43 UTC on 23 September. (c) Source altitude of +EIP (red filled diamond) and the precursor +NBE (black asterisk) with the vertical profile of radar echo.

consisting of 63 −NBEs and 27 +EIPs, had sufficiently clear ground-ionosphere reflections to calculate the event source altitudes. Figure 2 shows (a) the −NBEs and +EIPs source altitudes with the time of day and source altitude distribution, (b) the source altitude of 20 −NBEs during a particular storm period, and (c) the source altitude of one +EIP following a lower +NBE.

The source altitude of 63 −NBEs ranged from 14.0 to 20.5 km (most of them clustered at 16–19 km), with a mean height of 17.8 km. Most of the −NBEs were produced by the thunderstorm on 23 September 2014 (Storm-Sep23, hereafter) and the thunderstorm on 3 October 2014 (Storm-Oct03, hereafter), which can also be illustrated from the two −NBEs temporal clusters in Figure 2a. For Storm-Sep23, the ground-based radar data illustrated the Enhanced Echo Top (EET, the maximum height of 18 dBZ radar reflectivity) is approximately 17–19 km, while the spaced-based IR cloud top temperature indicates a minimum IR cloud top temperature of less than −70°C. The high EETs and low cloud top temperature indicated an extremely strong convection during the −NBEs occurrence. −NBEs from Storm-Sep23 clustered at 16.6–18.6 km (only two occurred at 14.3 km and 14.6 km), which is consistent with previous reports as reviewed by *Lü et al.* [2013]. The −NBE source altitudes are comparable to the EETs, which was close to the storm tops. As illustrated in Figure 2b, 20 NBEs clustered at 17.2–18.3 km in two convective cells. Storm-Oct03 occurred in the middle of the Gulf of Mexico, so no ground-based radar was available. However, the IR cloud top temperature of Storm-Oct03 was at least 5°C cooler than that of Storm-Sep23, indicating even deeper convection during the −NBEs occurrence of Storm-Oct03. This resulted in a bit higher location of −NBEs, as illustrated in Figure 2a.

In contrast, all the 27 +EIPs occur below 13.5 km during the day and night. Most of +EIPs clustered from 10 to 13 km, with a mean height of 11.4 km, which is much lower than the −NBEs. Seventeen of the 27 +EIPs with reachable ground-based radar were found to be produced in storms with EETs ranging from 12.2 to 15.8 km. The vertical gaps between +EIP source altitudes and EETs were 0.1–3.8 km (three of them less than 0.7 km, all others greater than 1.0 km), with the mean and median value of 1.8 km. +EIPs thus occurred in the upper region but inside the thundercloud, and the convection of these thunderclouds was not as strong as those that generated −NBEs. Figure 2c illustrates a 243 kA +EIP that originated at 12.1 km, which occurred in a weaker convection cell compared to the −NBE-producing cells shown in Figure 2b. It is interesting to note that there is a 42 kA +NBE, with a source altitude of 8.0 km, that proceeded the +EIP by 3 ms, indicating the precursor lightning activity ahead of the +EIPs, as discussed in the following section.

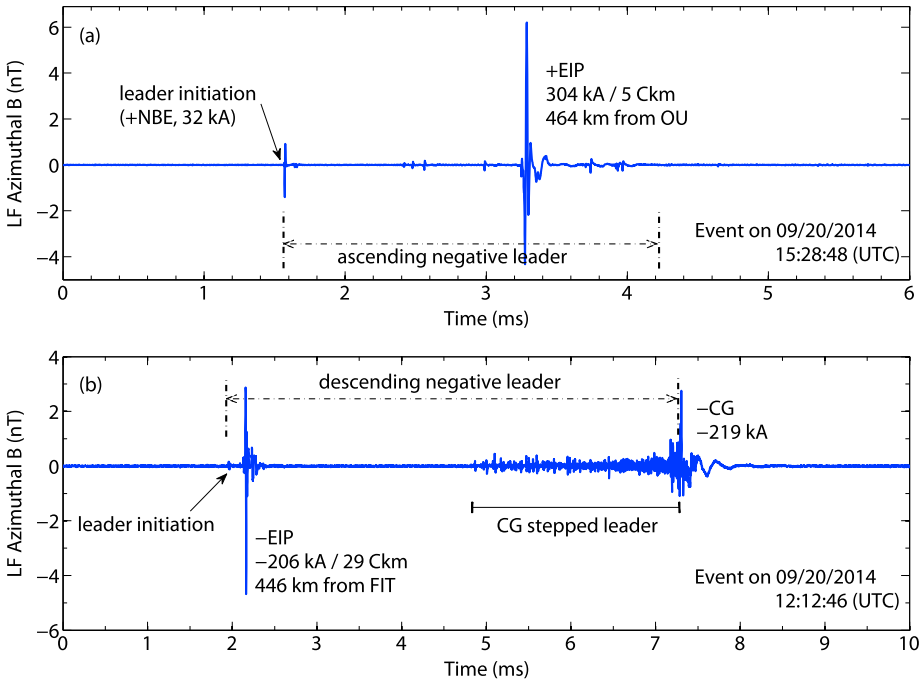

Figure 3. The temporal context of EIPs with normal lightning events. (a) A 304 kA +EIP with source altitude of 12.5 km generated during an ascending negative leader initiated by a 32 kA +NBE located at 7.9 km altitude. (b) −EIP generated during a descending negative leader followed by stepped leader and a negative CG stroke. The occurrence time of the events in the figure are given in UTC.

4. The Temporal Occurrence Context of EIPs With Normal Lightning Events

The coordinated NLDN and LF recordings provided us with useful clues about the temporal and spatial context of NBEs and EIPs with other normal lightning events. NBEs, especially −NBEs, usually occur in isolation. This means that no other events are detected within a few milliseconds of the NBE [*Smith et al.*, 1999]. However, all the EIPs (both positive and negative polarities) within a reasonable range from LF sensors were associated with detectable normal IC bipolar pulses within several milliseconds of them.

+EIPs usually appear within a few milliseconds after IC leader initiation. One specific situation is a +EIP generated during a negative IC leader initiated by a strong IC bipolar pulse, known to be a +NBE [*Le Vine*, 1980; *Smith et al.*, 1999], as shown in Figure 3a. The initiating +NBE (32 kA I_{pk}) was located at 7.9 km above the ground. After 1.6 ms, the +EIP occurred at height of 12.5 km, horizontally separated from the +NBE by 0.3 km (NLDN reported 50% geolocation error ellipse semimajor axis of 0.2 km for both events). Similarly, two more +EIPs that followed lower altitude +NBEs were also found. These two initiating +NBEs were located at 8.0 km and 7.8 km altitude, while the +EIPs were located at 12.1 km and 11 km, with the temporal interval of 3 ms and 2.5 ms between each pair of +NBE and +EIP, respectively. The horizontal separations between initiating +NBEs and +EIPs were 1.5 km and 0.6 km, with vertical separations of 4.1 km and 3.2 km.

The time interval of all initiating IC pulses (or +NBEs) and +EIPs ranges from 1 to 3 ms, with a mean time interval of 1.5 ms. It is known that +NBEs at lower altitude are capable of initiating an upward negative leader [*Rison et al.*, 1999; *Wu et al.*, 2014]. The intimate temporal and spatial relationship between the initiating +NBEs/IC pulses and +EIPs demonstrates that +EIPs were generated during the upward negative leader processes initiated by the small +NBEs/IC pulses.

Only three −EIPs were recorded during this investigation. Similar to +EIPs, all of the −EIPs were associated with IC pulses before and after them. Time intervals between initiation pulses and −EIPs range in 0.2–0.5 ms, which are shorter than the typical time intervals between initiation pulse and +EIPs. In addition, all of the −EIPs were also followed by a sequence of pulse trains in several milliseconds. Specifically, one −EIP was followed by a pulse train (stepped leaders), which ended with a −CG return stroke, as illustrated in Figure 3b.

This 206 kA −EIP was followed by a 219 kA −CG, which was located 1.1 km from the −EIP. The −CG stepped leader started about 3 ms after the −EIP. The other two −EIPs with small iCMC (1 C km and 8 C km) were only followed by pulse trains which seemed to be attempted leader processes, but did not end with CG strokes.

For these three −EIPs, no source heights can be obtained, since no clear reflection pulses can be identified. Nevertheless, according to the close temporal-spatial relationship between −EIPs and the following pulse trains or CGs, we speculate that these −EIPs may be produced at a lower altitude than +EIPs. −EIPs are almost certainly produced during the early stages of downward negative leader processes. The downward negative leader sometimes ends with a −CG return stroke and sometimes does not.

From the NLDN reports, 25 of the 72 EIPs (both positive and negative polarities) followed NLDN-reported ICs (7–45 kA I_{pk}). The LF waveforms also showed that other EIPs with non-NLDN-reported preceding ICs do associate with IC pulses, even though no exact spatial contexts can be obtained. It is indicated that there are IC pulses both before and after the EIPs within a few milliseconds, regardless of the polarity of the EIPs. This is different from the occurrence context of NBEs [*Smith et al*., 1999; *Rison et al*., 1999; *Wu et al*., 2014], from which it also indicates the distinction of physical mechanisms of themselves.

5. Discussion and Summary

With the goal of understanding the nature of very high peak current IC lightning events, we analyzed the LF radio emissions from 199 NLDN-identified IC events with reported I_{pk} above 200 kA. This data set contained three distinct classes of lightning event that we showed are quantitatively distinguishable based on details of their LF waveforms: CG lightning strokes, in-cloud NBEs (especially −NBEs), and what we call energetic in-cloud pulses or EIPs. NBEs have received a great deal of attention since the identification by *Le Vine* [1980] and characterization by *Smith et al*. [1999], while EIPs have not previously been reported as a distinct class of in-cloud lightning event. The NLDN-reported I_{pk} of NBEs and EIPs analyzed in this study are comparable and ranged from 200 to 304 kA and 200 to 584 kA, respectively. But, the significant difference in their LF waveforms and their occurrence contexts demonstrates that NBEs and EIPs are two distinct types of energetic IC events produced by different physical mechanisms.

The measured source altitudes indicated the meteorology environmental contexts of −NBEs and +EIPs. Most of the −NBEs were generated at 16–19 km, with a mean height of 17.8 km. The enhanced echo top of these −NBE-producing storms reached 17–19 km, which is often considered to be the strongest convection altitude during the storms. This places the −NBEs close to the storm tops and, based on their polarity, probably between the upper positive and negative screening charge layers. In contrast, the +EIPs were produced inside weaker thunderstorm convection. Most of the located +EIPs clustered at 10–13 km, with a mean height of 11.4 km. The mean space gap between +EIPs source altitude and enhanced echo top of the thunderclouds is about 1.8 km, placing them between the main negative and upper positive charge layers.

Clear IC pulses are seen within a few milliseconds before and after EIPs, and +EIPs often follow a lower altitude +NBE. This strongly suggests that EIPs occur after the initiation and during the propagation of a negative leader. Upward negative leaders can produce +EIPs, while (more rarely) downward negative leaders can produce −EIPs. In contrast, NBEs usually occur in isolation or serve as the initiation event of a leader process [*Rison et al*., 1999; *Wu et al*., 2014]. These different occurrence contexts also point to different physical mechanisms of NBEs and EIPs. +EIPs are produced approximately 1–3 ms after upward negative leader initiation, while −EIPs are produced only 0.2–0.5 ms after downward negative leader initiation. Interestingly, the downward negative leaders that produce −EIPs do not always end with a −CG stroke.

The different time intervals from leader initiation to EIP production point to a possible influence in their generation. That −EIPs are produced very quickly after downward negative leader initiation suggests that they are produced in high local electric fields that are present near the initiation point but absent once the leader exits the cloud. Upward negative leaders propagating between the main negative and upper positive charge layers experience high electric fields over a longer vertical range. If high local electric fields are required for EIP production, then we would expect +EIPs to be produced in a wider range of times from leader initiation, and this is precisely what is observed. While this suggests that high local electric fields are part of EIP production, it is not clear whether EIPs are simply an extremely energetic negative leader step, or whether they are produced by a fundamentally different process triggered by the negative leader tip.

The occurrence context of EIPs is comparable to the terrestrial gamma ray flash (TGF) observed by lightning mapping array [*Lu et al.*, 2010]. In at least one instance, a previously reported TGF was simultaneous with what this work identifies as a +EIP [*Cummer et al.*, 2014], in terms of pulse shape, source altitude, and lightning leader context. This indicates that there is likely some connection between EIPs and TGFs. If this connection is robust (and more investigation is clearly required), then the existence of both polarities of EIP shown here suggests the possibility of downward TGFs produced in association with descending negative leaders in high upward pointing electric field regions. The examples here suggest that such downward TGFs would be produced promptly (less than 0.5 ms) after the initiation of the downward leader.

Our analysis shows that IC events can produce radiated fields equivalent to I_{pk} as high as hundreds of kiloamperes (range in 200–584 kA), but with small iCMC. The small iCMC of NBEs and EIPs shows that they cannot produce sprites. However, the simulated results on the lightning electromagnetic pulse and its interaction with the lower ionosphere indicate the possible interaction between strong lightning discharges (both IC pulses and CG) and ionosphere [*Inan et al.*, 2010; *Marshall et al.*, 2010]. Our measurements indicated that the distant radiated fields from high I_{pk} IC events are comparable to those produced by strong CGs, and thus, these high I_{pk} events could generate elves [*Inan et al.*, 1991] and associated ionospheric perturbations [*Inan et al.*, 2010; *Marshall et al.*, 2010]. Elves are the ionosphere D-region optical signature of strong, polarity-independent coupling of lightning electromagnetic pulses with the ionosphere [*Inan et al.*, 1991; *Fukunishi et al.*, 1996; *Barrington-Leigh and Inan*, 1999] and simply require a sufficiently long-duration and high-amplitude electric field pulse in the ionosphere [*Barrington-Leigh and Inan*, 1999; *Kuo et al.*, 2007; *Chen et al.*, 2008]. The slower time scale of EIPs (typically 50–100 μs) in particular points to the possibility of elves being produced by EIPs and thus also the existence of a connection between elves and TGFs.

Acknowledgments

The authors would like to acknowledge support from the National Science Foundation Dynamic and Physical Meteorology program through grant ATM-1047588 and the DARPA Nimbus program through grant HR0011-10-1-0059. The authors also would like to acknowledge Gibson Ridge Software, LLC (GRS) and their product GR2Analyst on the radar data analyses. All data are available by request (cummer@ee.duke.edu), and the processing details are described fully in the manuscript.

The Editor thanks two anonymous reviewers for their assistance in evaluating this paper.

References

Barrington-Leigh, C. P., and U. S. Inan (1999), Elves triggered by positive and negative lightning discharges, *Geophys. Res. Lett.*, *26*, 683–686, doi:10.1029/1999GL900059.

Briggs, M. S., et al. (2010), A first results on terrestrial gamma ray flashes from the Fermi Gamma-ray Burst Monitor, *J. Geophys. Res.*, *115*, A07323, doi:10.1029/2009JA015242.

Chen, A. B., et al. (2008), Global distributions and occurrence rates of transient luminous events, *J. Geophys. Res.*, *113*, A08306, doi:10.1029/2008JA013101.

Cummer, S. A., and W. A. Lyons (2004), Lightning charge moment changes in U.S. High Plains thunderstorms, *Geophys. Res. Lett.*, *31*, L05114, doi:10.1029/2003GL019043.

Cummer, S. A., W. A. Lyons, and M. A. Stanley (2013), Three years of lightning impulse charge moment change measurements in the United States, *J. Geophys. Res. Atmos*, *118*, 5176–5189, doi:10.1002/jgrd.50442.

Cummer, S. A., M. S. Briggs, J. R. Dwyer, S. Xiong, V. Connaughton, G. J. Fishman, G. Lu, F. Lyu, and R. Solanki (2014), The source altitude, electric current, and intrinsic brightness of terrestrial gamma ray flashes, *Geophys. Res. Lett.*, *41*, 8586–8593, doi:10.1002/2014GL062196.

Cummins, K. L., and M. J. Murphy (2009), An overview of lightning locating systems: History, techniques, and data uses, with an in-depth look at the U.S. NLDN, *IEEE Trans. EMC*, *51*, 499–518, doi:10.1109/TEMC.2009.2023450.

Cummins, K. L., M. J. Murphy, E. A. Bardo, W. L. Hiscox, R. Pyle, and A. E. Pifer (1998), Combined TOA/MDF technology upgrade of U. S. National Lightning Detection Network, *J. Geophys. Res.*, *103*, 9035–9044, doi:10.1029/98JD00153.

Dwyer, J. R., D. M. Smith, and S. A. Cummer (2012), High-energy atmospheric physics: Terrestrial gamma-ray flashes and related phenomena, *Space Sci. Rev.*, *173*, 133–196, doi:10.1007/s11214-012-9894-0.

Fishman, G. J., et al. (1994), Discovery of intense gamma-ray flashes of atmospheric origin, *Science*, *264*, 1313–1316.

Franz, R. C., R. J. Nemzak, and J. R. Winkler (1990), Television image of a large upward electrical discharge above a thunderstorm system, *Science*, *249*, 48–51.

Fukunishi, H., et al. (1996), Elves: Lightning-induced transient luminous events in the lower ionosphere, *Geophys. Res. Lett.*, *23*, 2157–2160, doi:10.1029/96GL01979.

Inan, U. S., T. F. Bell, and J. V. Rodriguez (1991), Heating and ionization of the lower ionosphere by lightning, *Geophys. Res. Lett.*, *18*(4), 705–708, doi:10.1029/91GL00364.

Inan, U. S., S. A. Cummer, and R. A. Marshall (2010), A survey of ELF and VLF research on lightning-ionosphere interactions and causative discharges, *J. Geophys. Res.*, *115*, A00E36, doi:10.1029/2009JA014775.

Kuo, C. L., et al. (2007), Modeling elves observed by FORMOSAT-2 satellite, *J. Geophys. Res.*, *112*, A11312, doi:10.1029/2007JA012407.

Le Vine, D. M. (1980), Sources of the strongest RF radiation from lightning, *J. Geophys. Res.*, *85*, 4091–4095, doi:10.1029/JC085iC07p04091.

Lü, F., B. Zhu, H. Zhou, V. A. Rakov, W. Xu, and Z. Qin (2013), Observations of compact intracloud lightning discharges in the northernmost region (51N) of China, *J. Geophys. Res. Atmos.*, *118*, 4458–4465, doi:10.1002/jgrd.50295.

Lu, G., R. J. Blakeslee, J. Li, D. M. Smith, X.-M. Shao, E. W. McCaul, D. E. Buechler, H. J. Christian, J. M. Hall, and S. A. Cummer (2010), Lightning mapping observation of a terrestrial gamma-ray flash, *Geophys. Res. Lett.*, *37*, L11806, doi:10.1029/2010GL043494.

Lu, G., S. A. Cummer, J. Li, F. Han, D. M. Smith, and B. W. Grefenstette (2011), Characteristics of broadband lightning emissions associated with terrestrial gamma ray flashes, *J. Geophys. Res.*, *116*, A03316, doi:10.1029/2010JA016141.

Lu, G., et al. (2013), Coordinated observations of sprites and in-cloud lightning flash structure, *J. Geophys. Res. Atmos.*, *118*, 6607–6632, doi:10.1002/jgrd.50459.

Marshall, R. A., U. S. Inan, and V. S. Glukhov (2010), Elves and associated electron density changes due to cloud-to- ground and in-cloud lightning discharges, *J. Geophys. Res.*, *115*, A00E17, doi:10.1029/2009JA014469.

Rison, W., R. J. Thomas, P. R. Krehbiel, T. Hamlin, and J. Harlin (1999), A GPS-based three-dimensional lightning mapping system: Initial observations in central New Mexico, *Geophys. Res. Lett.*, *26*, 3573–3576, doi:10.1029/1999GL010856.

Smith, D. A., X. M. Shao, D. N. Holden, C. T. Rhodes, M. Brook, P. R. Krehbiel, M. Stanley, W. Rison, and R. J. Thomas (1999), A distinct class of isolated intracloud lightning discharges and their associated radio emissions, *J. Geophys. Res.*, *104*, 4189–4212, doi:10.1029/1998JD200045.

Smith, D. A., M. J. Heavner, A. R. Jacobson, X. M. Shao, R. S. Massey, R. J. Sheldon, and K. C. Wiens (2004), A method for determining intracloud lightning and ionospheric heights from VLF/LF electric field records, *Radio Sci.*, *39*, RS1010, doi:10.1029/2002RS002790.

Smith, D. M., L. I. Lopez, R. P. Lin, and C. P. Barrington-Leigh (2005), Terrestrial gamma-ray flashes observed up to 20 MeV, *Science*, *307*, 1085–1088, doi:10.1126/science.1107466.

Wiens, K. C., T. Hamlin, J. Harlin, and D. M. Suszcynsky (2008), Relationships among narrow bipolar events, "total" lightning, and radar-inferred convective strength in Great Plains thunderstorms, *J. Geophys. Res.*, *113*, D05201, doi:10.1029/2007JD009400.

Wu, T., S. Yoshida, T. Ushio, Z. Kawasaki, and D. H. Wang (2014), Lightning-initiator type of narrow bipolar events and their subsequent pulse trains, *J. Geophys. Res. Atmos.*, *119*, 7425–7438, doi:10.1002/2014JD021842.